DOI: 10.1002/chem.200902312

Cytotoxic Titanium Salan Complexes: Surprising Interaction of Salan and Alkoxy Ligands

Timo A. Immel, Ulrich Groth, and Thomas Huhn*[a]

Abstract: The synthesis, biochemical evaluation, and hydrolysis studies of a wide selection of alkyl- and halogen-substituted titanium salan alkoxides are presented herein. A systematic change in the employed alkoxides revealed that both the bulk of the salan ligands and the steric demand of the labile ligands are of great importance for the obtained biological activity. Surprisingly, these two factors are not independent from each other; lowering the steric demand of the alkoxide of a hitherto nontoxic complex renders it cytotoxic. Therefore, our data suggest that the overall size of the complex exerts a strong influence on its biological activity. To decide whether the correlation between the cytotoxicity and the steric demand of the whole complex is merely based on an altered hydrolysis or on the interaction with biomolecules, the behavior of selected complexes under hydrolytic conditions and the influence of transferrin were investigated. Complexes differing only in their labile alkoxy ligands gave the same hydrolysis products with similar hydrolysis rates but displayed cytotoxicities that differed in the range of one order of magnitude. Thus, it seems that the hydrolysis product is not the active species but rather that the unhydrolysed complex is important for the first interaction with a biomolecule. This promoted the idea of hydrolysis being a detoxification pathway. In accordance with the above conclusion, chloro-substituted complex $[Ti(Ph^{Cl}N^{Me})_2(O^{iPr})_2]$ displayed a high cytotoxicity ($IC_{50} \approx 5\ \mu M$) and surprisingly high hydrolytic stability ($t_{1/2} = 108$ h). These findings, together with the observed cytotoxicity in a cisplatin-resistant cell line, make halo-substituted salan complexes an interesting target for further studies.

Keywords: antitumor agents · cytotoxicity · hydrolysis · structure–activity relationships · titanium salan complexes

Introduction

Today, metal complexes, such as cisplatin, carboplatin, and oxaliplatin, play an important role in cancer therapy, but unfortunately the spectrum of activity of these platinum complexes is limited and they are associated with significant dose-limiting toxicities.[1–3] Therefore, much research has been devoted to the identification of new metal complexes with lower toxicity, similar antitumor activity, and reduced tumor resistance.[4–14] Titanium(IV) complexes showed encouraging antitumor activity in various cell lines and little cross resistance to cisplatin was observed.[15–17] Although much effort was undertaken to identify completely new titanium complexes that show antitumor properties, nearly all investigated complexes were derivatives of either titanocene dichloride ($[Ti(Cl_2)(Cp_2)]$)[18–22] or budotitane ($[Ti(bzac)_2(OEt)_2]$; Hbzac = phenylbutane-1,3-dione).[23–25]

One characteristic of the above-mentioned complexes is their very fast rate of hydrolysis that leads to unidentified products. In an aqueous environment, the loss of the labile groups occurs within seconds, whereas the more inert ligands hydrolyze on a timescale of hours or days.[26,27] On the one hand, this hampers the identification of the active species as well as the biological target and the mechanism of action. It was found that titanocene dichloride is enriched in

[a] T. A. Immel, Prof. Dr. U. Groth, Dr. T. Huhn
Fachbereich Chemie and
Konstanz Research School Chemical Biology
Universität Konstanz
Universitätsstrasse 10
Fach 720, 78457 Konstanz (Germany)
Fax: (+49) 7531-884424
E-mail: thomas.huhn@uni-konstanz.de

Supporting information for this article is available on the WWW under http://dx.doi.org/10.1002/chem.200902312, and contains synthetic procedures for the preparation of ligands and titanium complexes; detailed spectroscopic and analytical data for all new compounds; ^1H NMR spectra of complexes $[Ti(Ph^{Me}N^{Me})_2(O^{iPr})_2]$, $[Ti(Ph^{tBu}N^{Me})_2(O^{iPr})_2]$, $[Ti(Ph^{F}N^{Me})_2(O^{iPr})_2]$, $[Ti(Ph^{Cl}N^{Me})_2(O^{iPr})_2]$ and $[Ti(Ph^{Br}N^{Me})_2(O^{iPr})_2]$ at their respective $t_{1/2}$ values with overlaid spectra of the corresponding salans; details of the cytotoxicity assays and viability plots in Hep G2 for all compounds; color graphics for Figures 2–8 and Figures 11–12.

areas near the nuclear chromatin and covalently binds to DNA and inhibits DNA synthesis.[28–31] Titanocene dichloride was also reported to inhibit human topoisomerase II.[32] On the other hand, it is assumed that some ligand lability is necessary for the biological effect and that ligand hydrolysis leads to formation of the active species.

Concerning the cellular uptake, the role of ligand lability is controversial. Although it is necessary to strip off the ligands when Ti^{IV} is trafficked via transferrin,[33–37] a route via albumin could leave the complexes intact. An adduct of the complex stabilized by albumin might enter the cell, which would promote a more active role for these drugs in contrast to the prodrug role proposed for the transferrin delivery mechanism.[38]

Consistent with these findings, in 2007 two methyl substituted titanium salan complexes were reported to be cytotoxic independent of transferrin.[39] By using a small collection of six alkyl-substituted titanium salan complexes, Tshuva and co-workers showed an influence due to the steric demand of the ligand and proposed a connection between the hydrolytic behavior of these complexes and their biological activity.[40–42] Exploring this third class of titanium complexes with antitumor activity, we could demonstrate that complexes of halogen-substituted salans in particular reveal promising biological properties. Their IC_{50} values are comparable to cisplatin and, in contrast to their alkyl-substituted congeners, they almost exclusively induce apoptotic cell death.[43]

Herein we describe the synthesis, biological evaluation, and hydrolytic behavior of a library of more than 40 alkyl- and halogen-substituted titanium salan complexes. The obtained data are discussed with respect to structure–activity relations and the influence of hydrolysis on cytotoxicity.

Results and Discussion

To elucidate the impact of both steric and electronic properties of the ligands on the antitumor activity and also the hydrolysis behavior, the synthesis of a small library of more than 40 different salan complexes was envisaged. For a systematic study, the influence of substituents on the aromatic rings and at the bridging nitrogen atoms of the salan as well as the role of the labile alkoxy ligands had to be addressed independently. To differentiate between electronic and steric influences, we decided to utilize a series of halogen-substituted phenols in the ligand preparation alongside different alkyl-substituted ones. Coupling these phenols with three different amino linkers allowed the systematic construction of amino-phenolato-ligands (salans). Thus, those ligands feature different steric bulk at the bridging nitrogen atoms and cover a broad range of electronic influences at the phenol moieties. Finally, employing four different titanium alkoxides ($[Ti(OEt)_4]$, $[Ti(OiPr)_4]$, $[Ti(OnBu)_4]$, $[Ti(OtBu)_4]$) in the complex formation allowed us to fine-tune the steric demand of the titanium-bound labile ligands as well.

The *o*,*p*-disubstituted salans were accessible by a Mannich condensation. Simple reflux of the appropriate substituted phenol, *N*,*N*′-dialkylethylenediamine, and formaldehyde in methanol gave ligands $(Ph^{b–f}N^{a–c})_2$ in moderate yield as shown in Scheme 1.[43–45] In the case of aryl unsubstituted ligand $(Ph^{H}N^{Me})_2$, salicylaldehyde was reacted with ethylenediamine, then the resulting imine was reduced with sodium borohydride and subsequently methylated by reductive amination to give the desired salan.[46] Finally, metalation of these salans with different titanium alkoxides $Ti(O^{a–d})_4$, as shown in Scheme 2, gave titanium(IV) salan complexes

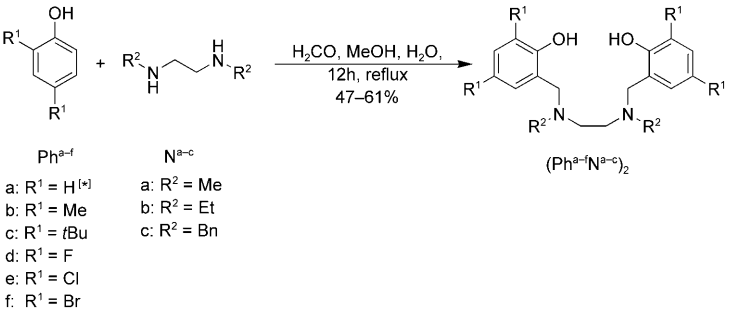

Scheme 1. Synthesis of salan ligands by Mannich condensation.[43–45] [*] Salans with $R^1=H$ were not accessible by this synthesis and were instead synthesized according to a published procedure.[46]

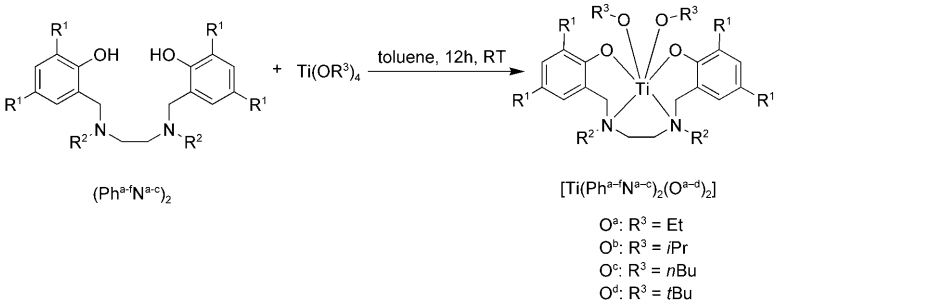

Scheme 2. Synthesis of titanium salan complexes by metalation with different titanium alkoxides.[43,46,47]

$[Ti(Ph^{a–f}N^{a–c})_2(O^{a–d})_2]$ in nearly quantitative yield as single (racemic) isomers.[43,47] To remove trace impurities, all compounds were recrystallized at least once prior to cytotoxicity studies. Purities were proven by combustion analysis.

All of the complexes described above were tested for antitumor behavior by using the well-established AlamarBlue assay, which is known to be highly reproducible and more sensitive than the MTT assay.[48] The cytotoxicity was studied in two different cell lines: the human cervix carcinoma cell line HeLa S3 and the Hep G2 cell line, an established human hepatocarcinoma cell line with epithelial morphology.[43] Cisplatin was used as a reference substance in all

assays. It showed an IC_{50} of (1.2 ± 0.4) μM in HeLa S3 and (3.0 ± 1.3) μM in Hep G2 cells. All IC_{50} values are given as mean values from at least three independent experiments each done in four replicates.

Selected complexes were subject to time-resolved hydrolysis studies monitored by NMR spectroscopy to assess their stability under biologically relevant conditions. We were especially interested in the influence of electronic features at the salan ligand (halogen vs. alkyl) on the speed and product formation of hydrolysis. Furthermore, the impact of steric crowding around the metal center and its effect on hydrolysis was paid special attention by utilizing alkoxides with differing steric demands.

Table 1. Selected bond lengths [Å] and angles [°] for a series of complexes with different alkoxides.

	$[Ti(Ph^{Me}N^{Me})_2(O^{Et})_2]$	$[Ti(Ph^{Me}N^{Me})_2(O^{nBu})_2]$	$[Ti(Ph^{Me}N^{Me})_2(O^{tBu})_2]$
O1–Ti1	1.8964(18)	1.8937(13)	1.923(3)
O2–Ti1	1.8977(18)	1.9086(13)	1.903(3)
O3–Ti1	1.8300(19)	1.8209(13)	1.780(2)
O4–Ti1	1.8328(19)	1.8226(13)	1.779(3)
N1–Ti1	2.342(2)	2.3392(16)	2.371(3)
N2–Ti1	2.336(2)	2.3214(14)	2.365(3)
O3-Ti1-O4	104.60(9)	105.95(6)	108.78(12)
O3-Ti1-O1	94.96(9)	97.03(6)	95.90(11)
O4-Ti1-O1	92.50(8)	93.58(6)	92.34(12)
O3-Ti1-O2	92.71(8)	89.45(5)	93.18(11)
O4-Ti1-O2	95.97(8)	96.06(6)	96.99(12)
O1-Ti1-O2	166.78(8)	166.46(6)	164.16(11)
O3-Ti1-N2	164.54(8)	164.25(6)	162.30(13)
O4-Ti1-N2	90.29(8)	88.13(6)	88.50(12)
O1-Ti1-N2	88.41(8)	88.92(5)	86.94(11)
O2-Ti1-N2	81.43(8)	81.93(5)	80.57(11)
O3-Ti1-N1	90.20(8)	90.36(6)	89.31(11)
O4-Ti1-N1	164.27(9)	163.21(6)	161.01(12)
O1-Ti1-N1	80.72(8)	80.21(5)	79.70(11)
O2-Ti1-N1	88.51(8)	87.90(5)	87.48(11)
N2-Ti1-N1	75.43(8)	76.24(5)	73.98(11)

As revealed by the ^{1}H NMR spectra, the geometrical features of the tetradentate [ONNO]-type ligands in all of our complexes are in general very similar. The N-CH_2CH_2-N methylene and the benzylic protons showed the familiar AB pattern consistent with C_2 symmetry and a *fac–fac* wrapping mode.[49] To compare the influence of the two monodentate ligands on complex geometry, a series of complexes with different labile alkoxides ($[Ti(Ph^{Me}N^{Me})_2(O^{a,c,d})_2]$) was closely investigated. Suitable crystals for X-ray structure determination were either grown by slow diffusion of hexane into a saturated solution in toluene ($[Ti(Ph^{Me}N^{Me})_2(O^{nBu})_2]$) or directly from hexane solutions at room temperature by slow evaporation ($[Ti(Ph^{Me}N^{Me})_2(O^{Et})_2]$, $[Ti(Ph^{Me}N^{Me})_2(O^{tBu})_2]$). The X-ray structures of this complex series again revealed the typical geometry of C_2-symmetrical complexes with very similar structural features. With the labile alkoxy ligands bound at the equatorial plane in a *cis* fashion and both phenolates occupying the bis-*trans*-axial positions, the complexes exhibit only minor differences in bond length and angles. With a slightly shorter Ti–alkoxide bond (1.78 Å) compared with complexes with unbranched alkoxides, $[Ti(Ph^{Me}N^{Me})_2(O^{tBu})_2]$ is different to the others members of this series (1.82–1.83 Å). This is compensated by a longer Ti–N bond of 2.37 Å as compared with 2.32–2.34 Å for the other series members, which results in a smaller phenolate-Ti-phenolate (O-Ti-O) angle of 164.16° compared with 166.46-166.78° for the other members of this class of complexes (Table 1, Figure 1). For $[Ti(Ph^{Me}N^{Me})_2(O^{Et})_2]$, the H atoms of all methyl groups were found to be disordered by a rotation of 60° and were, therefore, refined to fix the occupancies at 0.5 each. In $[Ti(Ph^{Me}N^{Me})_2(O^{tBu})_2]$, one of the *tert*-butoxy groups was found to be disordered over two sites with occupancies of 0.675 and 0.325. The methyl groups of the second *tert*-butoxy group showed rotational disorder and were refined as described above, which resulted in a higher *R*-factor of 6.97. A summary of experimental crystal data for all determined structures is given in the Experimental Section (Table 9).

Titanium-bound alkoxides

Influence on cytotoxicity in alkylsalans: Cytotoxicity studies done in the late 1980s by Köpf-Maier et al. with titanocenes with different labile ligand substitutions showed the negligible influence on cytotoxicity.[50] The question as to whether the influence of labile ligands is more pronounced in the case of titanium salan complexes still remains open. Recent studies by Tshuva and co-workers that utilized catechol as a bidentate substitute for the isopropoxy groups showed a two-fold decrease in the cytotoxicity of the resulting complex.[40] Although the observed effect is significant, an explanation is not evident because not only is the steric influence altered, but also the exchange of the two monodentate isopropoxy groups for one bidentate catecholato ligand leads to a different complex geometry. In the starting complex the isopropoxy groups are oriented in a *cis* fashion, but the two phenolato substituents of the salan are now occupying their position, which results in a loss of symmetry. We decided to tackle the question of the labile ligands' influence on cytotoxicity by a more systematic approach. Therefore, in the first series of experiments the salan backbone was kept unchanged and instead the labile alkoxy ligands were permutated, in the hopes of keeping the complex symmetry unchanged.

To keep the probable steric influence as low as possible, the first set of salan complexes evaluated in the AlamarBlue assay consisted of the aryl-unsubstituted *N*-methylated ligands $(Ph^HN^{Me})_2$ metalated with titanium alkoxides $Ti(O^{a-c})_4$. The dose-response curves obtained with the HeLa S3 cell line for these three complexes ($[Ti(Ph^HN^{Me})_2$-

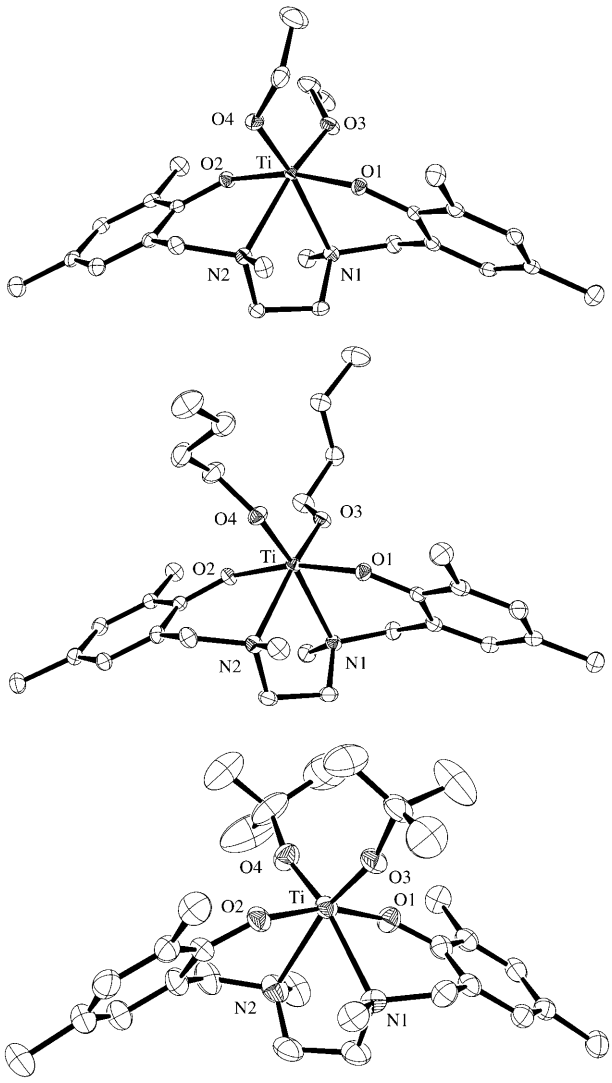

Figure 1. ORTEP diagram of the molecular structures of complexes [Ti(Ph^{Me}N^{Me})$_2$(O^{Et})$_2$] (top), [Ti(Ph^{Me}N^{Me})$_2$(O$^{n Bu}$)$_2$] (middle), and [Ti(Ph^{Me}N^{Me})$_2$(O$^{t Bu}$)$_2$] (bottom). Displacement ellipsoids are drawn at the 50% probability level. Main occupancy is shown for disordered groups; hydrogen atoms are omitted for clarity.

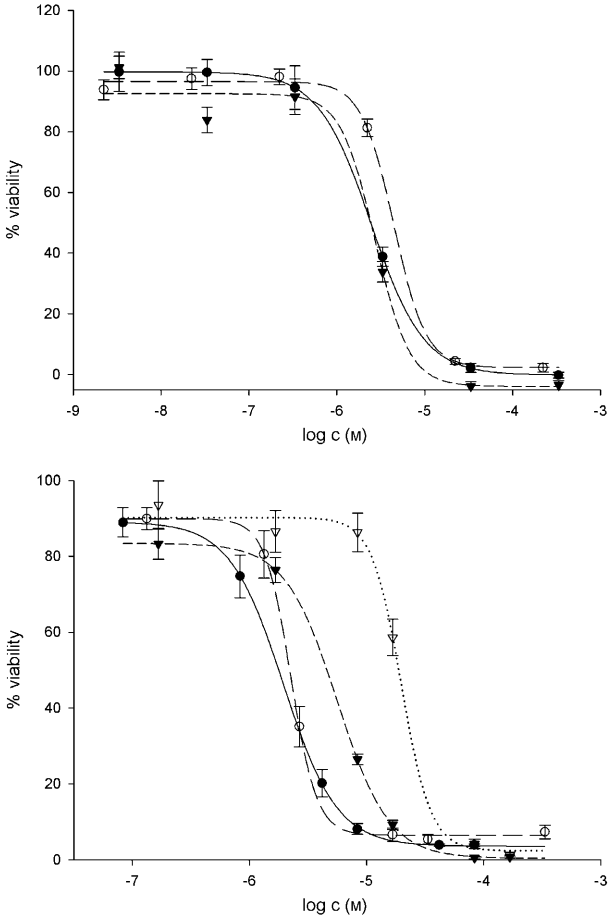

Figure 2. Viability of Hela S3 cells after incubation for 48 h with top: [Ti(Ph^{H}N^{Me})$_2$(O^{Et})$_2$] (●), [Ti(Ph^{H}N^{Me})$_2$(O$^{i Pr}$)$_2$] (○), [Ti(Ph^{H}N^{Me})$_2$(O$^{n Bu}$)$_2$] (▼) and bottom: [Ti(Ph^{Me}N^{Me})$_2$(O^{Et})$_2$] (●), [Ti(Ph^{Me}N^{Me})$_2$(O$^{i Pr}$)$_2$] (○), [Ti(Ph^{Me}N^{Me})$_2$(O$^{n Bu}$)$_2$] (▼), [Ti(Ph^{Me}N^{Me})$_2$(O$^{t Bu}$)$_2$] (▽). Dose-response curves were measured by using an AlamarBlue assay and show the dependence on the steric bulk of labile ligands in complexes with an unchanged [ONNO]-backbone.

(O$^{a–c}$)$_2$]) showed IC$_{50}$ values of 2.5–4.5 μM (Figure 2a). This lies in the range of the already known complex [Ti(Ph^{Me}N^{Me})$_2$(O$^{i Pr}$)$_2$].[39,43] Interestingly, the permutation of the labile alkoxy ligands had virtually no effect on the cytotoxicity of the three different complexes [Ti(Ph^{H}N^{Me})$_2$(O$^{a–c}$)$_2$].

Unexpectedly, we did observe a clear influence due to the labile ligands when testing the second set of four complexes ([Ti(Ph^{Me}N^{Me})$_2$(O$^{a–d}$)$_2$]). With methyl groups at positions two and four of the phenolato substituents of the salan backbone, they feature slightly increased steric crowding around the metal center and an enlarged overall steric demand. This influence on cytotoxicity is especially pronounced when comparing the bulky *tert*-butoxy-substituted [Ti(Ph^{Me}N^{Me})$_2$(O$^{t Bu}$)$_2$] with its less hindered ethoxy congener. A noteworthy 10-fold decrease in cytotoxicity was observed (Figure 2b).

In the third set of the alkyl series, the 2,4-di-*tert*-butyl-substituted salan was employed. Its titanium isopropoxy complex, [Ti(Ph$^{t Bu}$N^{Me})$_2$(O$^{i Pr}$)$_2$], is known to be nontoxic. Based on the above results of the [Ti(Ph^{Me}N^{Me})$_2$(O$^{a–d}$)$_2$] complexes, we initially hoped to regain cytotoxicity by reducing the steric demand of the employed alkoxide. But even when the smaller, non-branched ethoxide was used as the labile ligand, the resulting [Ti(Ph$^{t Bu}$N^{Me})$_2$(O^{Et})$_2$] complex remained nontoxic. An attempt to synthesize [Ti(Ph$^{t Bu}$N^{Me})$_2$(O$^{t Bu}$)$_2$] failed, possibly due to steric interference of the labile ligands and the salan backbone.

Table 2 summarizes the IC$_{50}$ values of these titanium salan complexes in both HeLa S3 and Hep G2 cells.

Influence on cytotoxicity in halogen-substituted salans: It is known that halogen-aryl-substituted salan complexes of titanium show a favorable biological profile.[43] For this reason as well as the gradual change in electronic and steric influences, a group of complexes that have fluoro, chloro and bromo substituents at the aromatic moiety was examined.

Table 2. IC_{50} [μM] values in Hela S3 and Hep G2 cells after incubation for 48 h with complexes $[Ti(Ph^{a-c}N^{Me})_2(O^{a-d})_2]$, as measured by using an AlamarBlue assay.

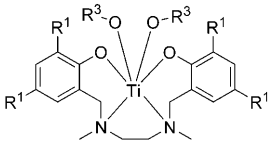

	Hela S3			Hep G2		
	$R^1=H$	$R^1=Me$	$R^1=tBu$	$R^1=H$	$R^1=Me$	$R^1=tBu$
$R^3=Et$	2.5±0.4	2.0±0.3	nontoxic	5.2±1.3	1.6±0.3	nontoxic
$R^3=iPr$	4.5±1.3	2.3±0.1	nontoxic	5.5±1.9	2.1±0.1	nontoxic
$R^3=nBu$	2.7±0.7	5.6±0.5	nontoxic	4.4±2.6	5.2±0.5	nontoxic
$R^3=tBu$	–	19.8±2.4	–	–	26.9±8.6	–

Again, changing the alkoxide while keeping the backbone unchanged should reveal the influence of steric interference on the IC_{50}. This may offer the possibility of fine-tuning the biological properties of such complexes.

In the case of the fluoro-substituted salan $[Ti(Ph^FN^{Me})_2(O^{a-c})_2]$ complexes, changing the alkoxy ligands had virtually no effect on the activity (Figure 3a) and resembles the $[Ti(Ph^HN^{Me})_2(O^{a-c})_2]$ case in this respect. All three complexes had their IC_{50} value within a very narrow margin of 1.3 to 1.6 μM.

In the chloro-substituted salan set of complexes, a strong influence on the observed cytotoxicity due to the bulkiness of the labile alkoxy ligand was observed (Figure 3b). The complex with an ethoxy group had a more than 40-fold higher cytotoxicity in HeLa S3 cells as compared with its *tert*-butoxy congener, which shows that the effect was even more pronounced than in the case of complexes $[Ti(Ph^MeN^{Me})_2(O^{a-d})_2]$.

For the most sterically demanding bromo-substituted salan backbone $(Ph^{Br}N^{Me})_2$, a tremendous decrease in cytotoxicity was observed for complexes with the more sterically demanding alkoxides (Figure 3c), with the *tert*-butoxide complex being completely nontoxic.

The IC_{50} values of all halogen-bearing titanium salan complexes $[Ti(Ph^{d-f}N^{Me})_2(O^{a-d})_2]$ are summarized in Table 3.

Table 3. IC_{50} [μM] values obtained for the $[Ti(Ph^{d-f}N^{Me})_2(O^{a-d})_2]$complexes by using the AlamarBlue assay with Hela S3 and Hep G2 cells. The cells were incubated with the complexes for 48 h prior measurement.

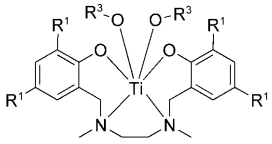

	Hela S3			Hep G2		
	$R^1=F$	$R^1=Cl$	$R^1=Br$	$R^1=F$	$R^1=Cl$	$R^1=Br$
$R^3=Et$	1.3±0.4	1.0±0.2	1.3±0.4	1.8±0.3	1.9±0.3	1.5±0.6
$R^3=iPr$	1.6±0.1	5.3±0.2	13±1	2.2±0.1	4.0±0.2	40±6
$R^3=nBu$	1.4±0.6	8.4±2.0	45.5±5.8	1.5±0.4	14.6±6.0	83.6±33.5
$R^3=tBu$	–	41.4±6.6	nontoxic	–	53.2±14.5	nontoxic

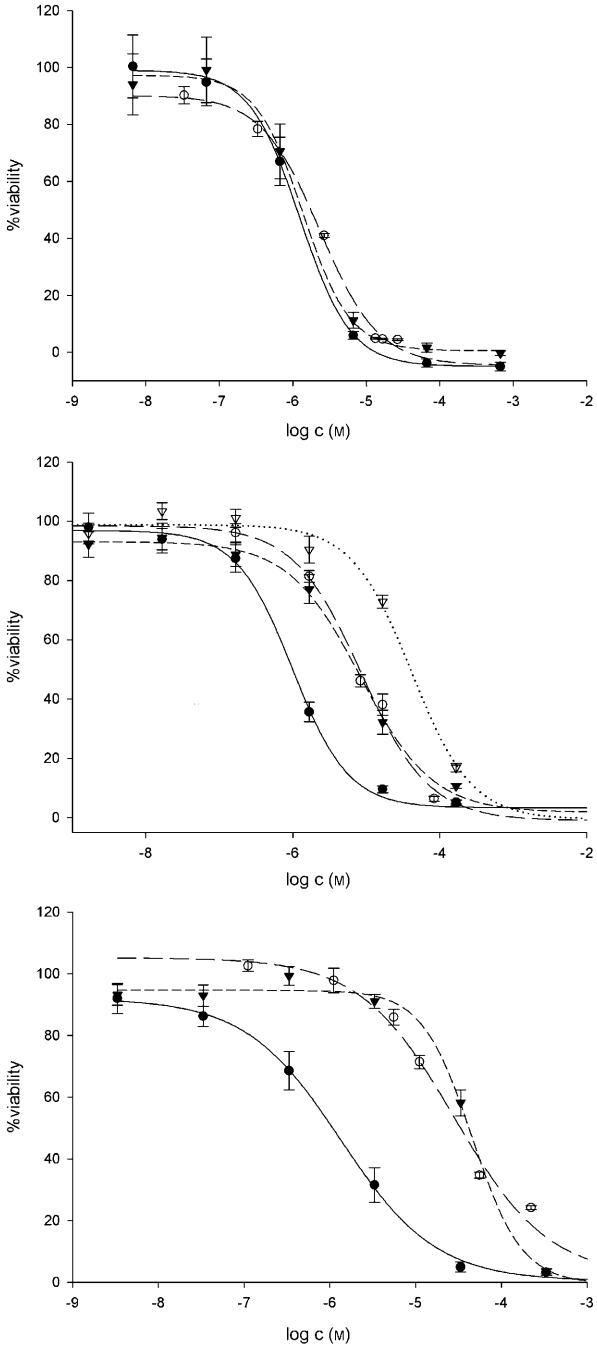

Figure 3. Viability of Hela S3 cells after incubation for 48 h with top: $[Ti(Ph^FN^{Me})_2(O^{Et})_2]$ (●), $[Ti(Ph^FN^{Me})_2(O^{iPr})_2]$ (○), $[Ti(Ph^FN^{Me})_2(O^{nBu})_2]$ (▼); middle: $[Ti(Ph^ClN^{Me})_2(O^{Et})_2]$ (●), $[Ti(Ph^ClN^{Me})_2(O^{iPr})_2]$ (○), $[Ti(Ph^ClN^{Me})_2(O^{nBu})_2]$ (▼), $[Ti(Ph^ClN^{Me})_2(O^{tBu})_2]$ (▽); and bottom: $[Ti(Ph^BrN^{Me})_2(O^{Et})_2]$ (●), $[Ti(Ph^BrN^{Me})_2(O^{iPr})_2]$ (○), $[Ti(Ph^BrN^{Me})_2(O^{nBu})_2]$ (▼). Dose-response curves were obtained by using an AlamarBlue assay.

To elucidate the influence of transferrin on the cytotoxicity of the halogen-substituted salan complexes, human apotransferrin was added to the medium prior to incubation of selected complexes. For alkyl-substituted salans, it has already been shown that the cell penetration mechanism is independent of transferrin.[40] Remarkably, even though the mechanism of action seems to be different for halogen-sub-

stituted complexes,[43] their cytotoxicity was not altered upon addition of human apo-transferrin (Figure 4).

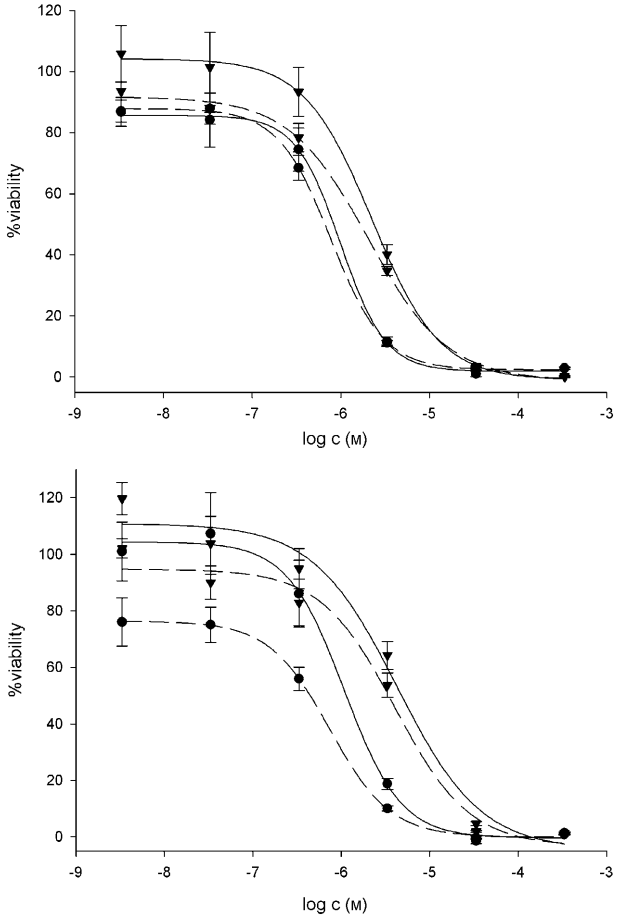

Figure 4. Viability of Hela S3 cells (top) and Hep G2 cells (bottom) after incubation for 48 h with $[Ti(Ph^{F}N^{Me})_2(O^{iPr})_2]$ (●) and $[Ti(Ph^{Cl}N^{Me})_2(O^{iPr})_2]$ (▼) with (——) and without (– – –) added human apo-transferrin ($10\,mg\,mL^{-1}$).[51] Dose-response curves were obtained by using an AlamarBlue assay.

Concerning the mechanism of action of salan complexes, we were interested in whether they bear a resemblance to the well-explored mechanism of cisplatin. Therefore, $[Ti(Ph^{F}N^{Me})_2(O^{iPr})_2]$ was incubated with two different cell lines, one of which was cisplatin resistant (human bladder carcinoma, MGH-U1) and one of which was cisplatin hypersensitive (testicular germ-cell tumor, 833K). With sub-micromolar IC_{50} values of 0.5 ± 0.1 μM for MGH-U1 and 0.4 ± 0.1 μM for 833K, both cell lines showed a comparable sensitivity (Figure 5). This is an indication that titanium salan complexes and cisplatin differ in their mode of action.

The results of the halogen-substituted $[Ti(Ph^{d-f}N^{Me})_2(O^{a-d})_2]$ complexes with *N*-methylated salans show that both the bulk of the salan ligands and the size of the labile ligands are of great importance for the obtained biological activity.

In each series of complexes in which the salan is fixed and the alkoxide changed, the complex featuring the smallest

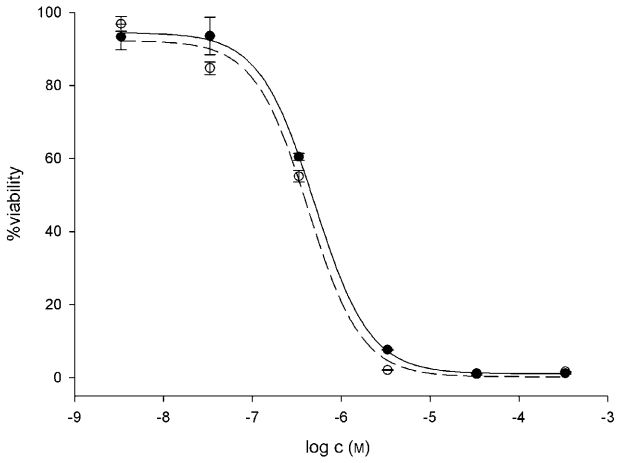

Figure 5. Viability of cisplatin-resistant (MGH-U1; ●) and cisplatin-hypersensitive (833K; ○) cells after incubation for 48 h with $[Ti(Ph^{F}N^{Me})_2(O^{iPr})_2]$. Dose-response curves were obtained by using an AlamarBlue assay.

alkoxide is the most toxic one. Moreover, it seems that these two factors are not independent from each other. The cytotoxicity of the sterically more demanding complexes of $(Ph^{Cl,Br}N^{Me})_2$ is more strongly affected by an additional bulky labile ligand than is the complex of $(Ph^{F}N^{Me})_2$ with only small fluoro substituents at the salan backbone. It is evident that the influence of the steric demand of the labile alkoxy ligands increases with the size of the halogen at the backbone.

This result also gives an explanation as to why the cytotoxicity of $[Ti(Ph^{Me}N^{Me})_2(O^{a-d})_2]$ is dependent on the alkoxy ligands in the earlier set of alkyl-substituted titanium salan complexes, whereas it is not for the unsubstituted $[Ti(Ph^{H}N^{Me})_2(O^{a-c})_2]$ complexes.

It seems that cytotoxicity does not depend solely on either the steric demand of the salan backbone or the bulkiness of the alkoxide used. In fact, quite the contrary seems to hold true. Complexes with small substituents at the aromatic rings ($[Ti(Ph^{H,F}N^{Me})_2(O^{a-d})_2]$) show no decreased IC_{50} even with the bulky *tert*-butoxide as the labile ligand. The smallest increase in steric demand on the side of the backbone leads to a stepwise decreased cytotoxicity of the complex ($[Ti(Ph^{Me,Cl,Br}N^{Me})_2(O^{a-d})_2]$), which depends on the bulkiness of the alkoxide used. Being independent from the nature of the employed substituent, alkyl or halogen, this effect appears not to be of electronic origin but rather based on the sheer size of the involved groups. Seemingly, there is something like an upper threshold, from where on the whole complex loses its cytotoxicity. To verify this conclusion, we decided to synthesize another series of complexes with additional steric hindrance at the bridging nitrogen atoms of the salan backbone.

Steric influence at the bridging nitrogen atoms

Cytotoxicity of N-ethylated complexes: Recently it has been reported that in the case of a salan ligand with two methyl

groups at each aromatic ring, exchange of the methyl at the bridging nitrogen atoms by an ethyl group resulted in a complete loss of toxicity of the corresponding bis(isopropoxy)titanium complex.[40] Therefore, we were interested in restoring the cytotoxicity of similar complexes just by lessening the steric demand of the alkoxide groups.

A first set of *N*-ethylated complexes was, therefore, prepared by metalating the dimethyl salan ligand $(Ph^{Me}N^{Et})_2$ with four different titanium alkoxides $Ti(O^{a-d})_4$ with different steric demands. In accordance with results published for a very similar complex,[40] we found $[Ti(Ph^{Me}N^{Et})_2(O^{iPr})_2]$ to be nontoxic. As expected, in the case of complexes $[Ti(Ph^{Me}N^{Et})_2(O^{nBu})_2]$ and $[Ti(Ph^{Me}N^{Et})_2(O^{tBu})_2]$ cytotoxicity was also not observed, presumably due to the even bulkier labile alkoxides adding to the overall size. In the much more interesting case of the $[Ti(Ph^{Me}N^{Et})_2(O^{Et})_2]$ complex with reduced steric demand from the alkoxide, we could indeed restore cytotoxicity in both cell lines used. With an IC_{50} value of $\approx$25 μM in HeLa S3 and Hep G2 cells it showed a mediocre biological activity, being one order of magnitude less than the most toxic complexes (Table 4).

Table 4. IC_{50} [μM] values obtained for the $[Ti(Ph^{d-f}N^{Et})_2(O^{a-d})_2]$ complexes in Hela S3 and Hep G2 cells. The cells were incubated with the complexes for 48 h prior to measurement.

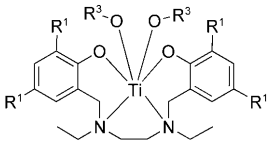

	Hela S3			Hep G2		
	R^1=Me	R^1=F	R^1=Cl	R^1=Me	R^1=F	R^1=Cl
R^3=Et	25.0±6.7	2.7±0.6	2.9±0.8	24.4±8.7	4.9±0.9	3.4±0.9
R^3=*i*Pr	nontoxic	2.3±0.4	7.1±1.7	nontoxic	2.5±1.1	14.3±4.0
R^3=*n*Bu	nontoxic	4.9±0.9	239.0±41.1	nontoxic	5.7±1.6	256.6±82.7
R^3=*t*Bu	nontoxic	–	nontoxic	nontoxic	–	nontoxic

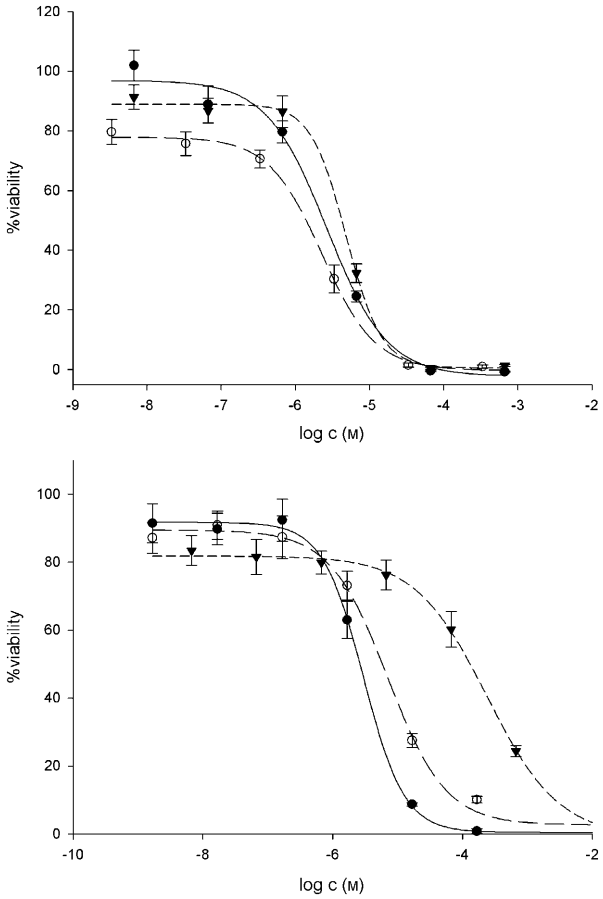

Figure 6. Viability of Hela S3 cells after incubation for 48 h with fluoroaryl *N*-ethyl-bridged complexes $[Ti(Ph^FN^{Et})_2(O^{a-c})_2]$ (top; ●: $[Ti(Ph^FN^{Et})_2(O^{Et})_2]$, ○: $[Ti(Ph^FN^{Et})_2(O^{iPr})_2]$, ▼: $[Ti(Ph^FN^{Et})_2(O^{nBu})_2]$) and chloroaryl *N*-ethyl-bridged complexes $[Ti(Ph^{Cl}N^{Et})_2(O^{a-c})_2]$ (bottom; ●: $[Ti(Ph^{Cl}N^{Et})_2(O^{Et})_2]$, ○: $[Ti(Ph^{Cl}N^{Et})_2(O^{iPr})_2]$, ▼: $[Ti(Ph^{Cl}N^{Et})_2(O^{nBu})_2]$), which demonstrate the dependence on the steric demand of the labile ligand in complexes with an unchanged *N*-ethyl backbone. Dose-response curves were obtained by using an AlamarBlue assay. The $[Ti(Ph^{Cl}N^{Et})_2(O^{tBu})_2]$ complex was nontoxic.

Encouraged by this finding, we turned our attention towards the electron-deficient fluoro- and chloro-substituted complexes with *N*-ethyl groups $[Ti(Ph^{d,e}N^{Et})_2(O^{a-d})_2]$. As shown in Figure 6a, all complexes resulting from metalation of the sterically less demanding fluoro-substituted ligand $(Ph^FN^{Et})_2$ showed similar IC_{50} values in the range of 2.3 to 4.9 μM, even with the bulkiest titanium alkoxide. It seems that the critical overall size for a significant decrease in toxicity cannot be reached within this specific set of ligands. A completely different situation revealed a series of chloro-substituted salan complexes, $[Ti(Ph^{Cl}N^{Et})_2(O^{a-d})_2]$. A tremendous effect on cytotoxicity that depended on the size of the alkoxide used was observable (Figure 6b). With an IC_{50} value of 2.9 μM, complex $[Ti(Ph^{Cl}N^{Et})_2(O^{Et})_2]$ with a labile ethoxy ligand is highly toxic in HeLa S3 cells. With the increasing size of the utilized alkoxide, the respective complexes showed a stepwise decrease in cytotoxicity in both cell lines (Table 4). Whereas the isopropoxy complex is slightly less toxic with an IC_{50} value of 7.1 μM, $[Ti(Ph^{Cl}N^{Et})_2(O^{nBu})_2]$ already showed a biological activity that was decreased by more than two orders of magnitude. Finally, the *tert*-butoxy complex is completely nontoxic. This effect is even more pronounced than for the series of corresponding *N*-methylated complexes $[Ti(Ph^{Cl}N^{Me})_2(O^{a-d})_2]$ (Table 3).

The observed dependence of cytotoxicity on the alkoxides employed in the *N*-ethylated complexes $[Ti(Ph^{b,d,e}N^{Et})_2(O^{a-d})_2]$ and the intensification of this effect compared with the corresponding *N*-methylated complexes $[Ti(Ph^{b,d,e}N^{Me})_2(O^{a-d})_2]$ supports our hypothesis: The combined steric hindrance of salan and labile ligands is crucial for the anticancer activity of this class of titanium complexes.

On comparing both groups, we deduced the existence of a lower steric threshold; below this threshold, alteration of the overall steric demand either at the salan backbone or at the labile ligands has only a minor influence on cytotoxicity. This can be exemplified by varying the smallest of our complexes ($[Ti(Ph^FN^{Me})_2(O^{Et})_2]$). Minor variations of its salan backbone, either at the aromatic rings (F vs. Cl) or at the

bridging nitrogens (Me vs. Et) has virtually no influence on measured cytotoxicity. The same is true for variations of the labile ligands.

In all the above cases, a further reduction in size does not enhance cytotoxicity. The minimum IC_{50} values for such salan complexes seem to be in the region of 1 μM. When exceeding the lower steric threshold, even minor changes in steric demand have a tremendous effect on biological activity. This can be impressively demonstrated by comparing complexes $[Ti(Ph^{F}N^{Et})_2(O^{n Bu})_2]$ and $[Ti(Ph^{Cl}N^{Et})_2(O^{n Bu})_2]$. Replacing the small fluoro by a larger chloro substituent led to a 50-fold decrease in cytotoxicity. Exchanging methyl for ethyl at the bridging nitrogens of the highly toxic $[Ti(Ph^{Me}N^{Me})_2(O^{i Pr})_2]$ has an even more drastic effect because it led to the completely nontoxic $[Ti(Ph^{Me}N^{Et})_2(O^{i Pr})_2]$.

Concerning the influence of the alkoxy ligands on cytotoxicity, a simple change from ethoxy to *n*-butoxy led to a nearly 100-fold reduced toxicity for complexes $[Ti(Ph^{Cl}N^{Et})_2(O^{a,c})_2]$.

Toxicity is completely lost when a certain overall size is exceeded. For the *tert*-butoxy-substituted salan complexes, this upper steric threshold is already reached; even with small labile ligands, such as ethoxy ($[Ti(Ph^{t Bu}N^{Me})_2(O^{Et})_2]$), no toxicity was achieved.

Cytotoxicity of N-benzylated complexes: To explore the utmost tolerable steric demand at the bridging nitrogen atoms, we decided to introduce *N*-benzyl groups. For ease of comparison, we used the same phenols as in the *N*-Et case for the Mannich coupling. When tested for their cytotoxicity, only the least sterically hindered complex $[Ti(Ph^{F}N^{Bn})_2(O^{Et})_2]$ was cytotoxic at all, with an IC_{50} value of ≈10 μM in both cell lines (Table 5).

Table 5. IC_{50} [μM] values obtained for *N*-benzylated complexes measured in Hela S3 and Hep G2 cells after incubation for 48 h. Only the least bulky complex, $[Ti(Ph^{F}N^{Bn})_2(O^{Et})_2]$, displayed any cytotoxicity.

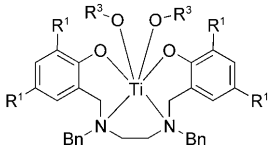

	Hela S3			Hep G2		
	R^1=Me	R^1=F	R^1=Cl	R^1=Me	R^1=F	R^1=Cl
R^3=Et	nontoxic	10.8±3.4	nontoxic	nontoxic	9.86±5.7	nontoxic
R^3=*i*Pr	nontoxic	nontoxic	nontoxic	nontoxic	nontoxic	nontoxic
R^3=*n*Bu	nontoxic	–	nontoxic	nontoxic	–	nontoxic
R^3=*t*Bu	–	–	nontoxic	–	–	nontoxic

As demonstrated above, the overall steric demand is the most important factor in determining biological activity. In a comparison of $[Ti(Ph^{F}N^{Bn})_2(O^{Et})_2]$ (the only *N*-benzylated complex to show any cytotoxicity) with its *N*-Me and *N*-Et congeners, the dose-response chart shows a stepwise decrease in cytotoxicity that again depends on the overall size of the respective complex (Figure 7).

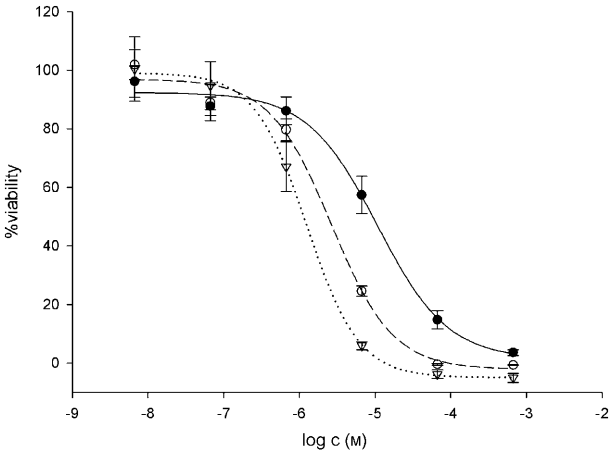

Figure 7. Viability of Hela S3 cells after incubation for 48 h with $[Ti(Ph^{F}N^{Me})_2(O^{Et})_2]$ (▽), $[Ti(Ph^{F}N^{Et})_2(O^{Et})_2]$ (○), and $[Ti(Ph^{F}N^{Bn})_2(O^{Et})_2]$ (●), showing the dependence on steric demand of the residue at the bridging nitrogens. Dose-response curves were obtained by using an AlamarBlue assay.

An analysis of all the measured biological data and comparison with the corresponding chemical structures elucidated interesting structure–activity relationships, that is, the obtained biological activity is not only dependent on the bulk of the salan ligands alone, but also on the steric hindrance of the labile ligands. Moreover, it seems that these two factors are not independent from each other because for bulky salan ligands an additional sterically hindered labile ligand is not tolerated. In fact, it leads to a strong decrease in or even a complete loss of cytotoxicity, whereas the same exchange of labile ligands does not affect the cytotoxicity of complexes with less sterically demanding salans.

The impact of this minute interplay of salan and labile ligand on cytotoxicity pointed us to the conclusion that the complex has to be intact at the particular moment when the steric bulk determines the cytotoxicity.

In contrast to titanocene complexes, not much is known about the specific mechanism of action of titanium salan complexes. Therefore, the question of at which point of interaction with its biological target the complex size matters still remains unanswered. In principle, the steric shielding around the titanium center influences stability, either against water alone or in conjunction with biomolecules, that is, transferrin or albumin. Considering the reaction with water, one might argue that the reduced or even absent toxicity of the bulky complexes might be explained by the following two scenarios: If the complex itself is toxic, then a higher steric demand at the titanium center might lead to a faster hydrolysis, thus generating nontoxic byproducts (detoxification mechanism). If the starting complex acts like a prodrug and is activated by hydrolysis, slower activation should lead to diminished or even absent toxicity (activation mechanism).

The decreased cytotoxicity of sterically demanding complexes might originate from inhibition of a specific interaction with biomolecules. This may affect their transport into

the cell, either by active transport via transferrin or by simple passive diffusion, the transfer to or the interaction with the cellular target. Experiments with added transferrin showed no significant influence on cytotoxicity, making an active cellular uptake via transferrin doubtable. If the uptake is based on diffusion, one might expect a faster transport of complexes featuring sterically demanding and, therefore, lipophilic side groups (*t*Bu, *N*-Bn, O-*t*Bu). Because those complexes show a diminished cytotoxicity in contrast to the ones with smaller and, therefore, more hydrophilic groups (F, Me, *N*-Me, O-Et), transport phenomena do not explain the size-dependent alteration of cytotoxicity.

Hydrolysis—Activation or deactivation mechanism? To elucidate whether the correlation of cytotoxicity and steric demand is merely based on an altered hydrolysis or depends on the interaction with biomolecules, we investigated the stability of several complexes upon the addition of a certain amount of water. We were interested in the influence the complex structure exerts on the speed of hydrolysis because this determines, besides the solubility, the applicability of such complexes in aqueous media. A systematic investigation of the life-time of such complexes under hydrolytic conditions with respect to their structure might, therefore, help to find substances with an improved pharmacological profile. Given that the fast formation of hydrolysis products has hampered mechanistic research for all titanium complexes found so far, stable and at the same time highly cytotoxic complexes would be valuable tools.

On the other hand, investigation of the hydrolysis process and the formed products might give insights into the role of hydrolysis in biological systems. Here it is interesting to ask whether hydrolysis is an activating or deactivating process. To obtain not only the rate of hydrolysis but also structural information about the products formed in aqueous media, we decided to follow the hydrolysis of our complexes by using time-resolved ^{1}H NMR spectroscopy in [D_8]THF/D_2O.[40]

The experiments were conducted in a mixture of [D_8]THF (95%), D_2O (4.8%), and DMSO (0.2%) at 37°C. To analyze the data, the decrease in at least two distinct signals of the titanium-bound salan backbone and the increase in the evolving signals of the free alkoxy ligands were monitored. The integrals were then normalized by using the DMSO signal as the internal standard and plotted against the hydrolysis time. Control measurements done in the absence of DMSO showed no significant differences in the hydrolysis rate and products formed. A complexation of the titanium center by the added standard could therefore be excluded. Keeping in mind that hydrolysis under in vivo conditions follows different rules, our impetus was merely to gather relative rates of hydrolysis. This allows us to determine which of our complexes is more and which is less stable in comparison to each other under given conditions.

In a first set of experiments, the influence of alterations at the aromatic moieties on the hydrolysis of our complexes was investigated. We were especially interested in the hydrolytic behavior of the halogen-substituted complexes [Ti(Ph^{d-f}N^{Me})$_2$(O^{iPr})$_2$] because these show favorable biological properties. In strong contrast to the alkylated complexes, they induce cell death by a purely apoptotic pathway. This might be due to a difference in hydrolysis, in respect to the rate or obtained products. For comparison, the highly cytotoxic alkyl complex [Ti(Ph^{Me}N^{Me})$_2$(O^{iPr})$_2$] and the nontoxic *tert*-butyl complex [Ti(Ph^{tBu}N^{Me})$_2$(O^{iPr})$_2$] were also tested (Figure 8).

Comparison of the hydrolytic half-life ($t_{1/2}$) of the investigated complexes (Table 6) revealed an interesting correlation: Within the alkyl-containing complexes [Ti(Ph^{b,c}N^{Me})$_2$(O^{iPr})$_2$], hydrolysis occurs faster with sterically demanding complexes. The opposite is true for the halogenated complexes ([Ti(Ph^{d-f}N^{Me})$_2$(O^{iPr})$_2$]). The methyl-substituted complex [Ti(Ph^{Me}N^{Me})$_2$(O^{iPr})$_2$] showed a $t_{1/2}$ value of 10 h, whereas in the *tert*-butyl case half of the complex had already decomposed 2 h after the initial water addition.

Table 6. Half-life of complexes [Ti(Ph^{b-f}N^{Me})$_2$(O^{iPr})$_2$] under hydrolytic conditions determined by time-resolved ^{1}H NMR spectroscopy at 37°C.

Complex	$t_{1/2}$ [h]	Complex	$t_{1/2}$ [h]
[Ti(Ph^{Me}N^{Me})$_2$(O^{iPr})$_2$]	10	[Ti(Ph^{F}N^{Me})$_2$(O^{iPr})$_2$]	6
[Ti(Ph^{tBu}N^{Me})$_2$(O^{iPr})$_2$]	2	[Ti(Ph^{Cl}N^{Me})$_2$(O^{iPr})$_2$]	108
		[Ti(Ph^{Br}N^{Me})$_2$(O^{iPr})$_2$]	>115

Under the chosen hydrolytic conditions, the bromo-substituted salan complex [Ti(Ph^{Br}N^{Me})$_2$(O^{iPr})$_2$] showed an impressive $t_{1/2}$ value of more than 115 h. It outruns its fluoro counterpart [Ti(Ph^{F}N^{Me})$_2$(O^{iPr})$_2$], which has a $t_{1/2}$ value of only 6 h, by a 20-fold increased hydrolytic stability. Unfortunately, this enormously stable complex displays only moderate biological activity. Surprisingly, the chloro-substituted salan complex showed a rather similar hydrolytic stability with a $t_{1/2}$ value of 108 h. This is remarkable because even though the stability is in the same range as the bromo counterpart, the biological activity is not. Compared with the most stable cytotoxic complex of this class known so far ([Ti(Ph^{Me}N^{Me})$_2$(O^{iPr})$_2$]),[41,42] the chloro complex showed a hydrolytic stability that was more than 10 times higher. A rather high toxicity ($IC_{50} \approx 5$ μM) and the fact that this complex exclusively induces apoptosis[43] makes it one of the most interesting substances with respect to mechanistic studies, and a promising candidate for further biological studies in the field of anticancer titanium complexes.

It has been observed by Peri et al. that upon hydrolysis [Ti(Ph^{tBu}N^{Me})$_2$(O^{iPr})$_2$] releases its salan ligand as well as the labile alkoxides. Hydrolysis of [Ti(Ph^{Me}N^{Me})$_2$(O^{iPr})$_2$] results in the formation of new species that possibly contain more than one titanium center. Careful examination of our data of the halogen-substituted complexes showed no liberation of free salan ligand upon hydrolysis. Instead, the ^{1}H NMR spectra showed the formation of new species with signals that indicated lower symmetry compared with the starting complex.[52]

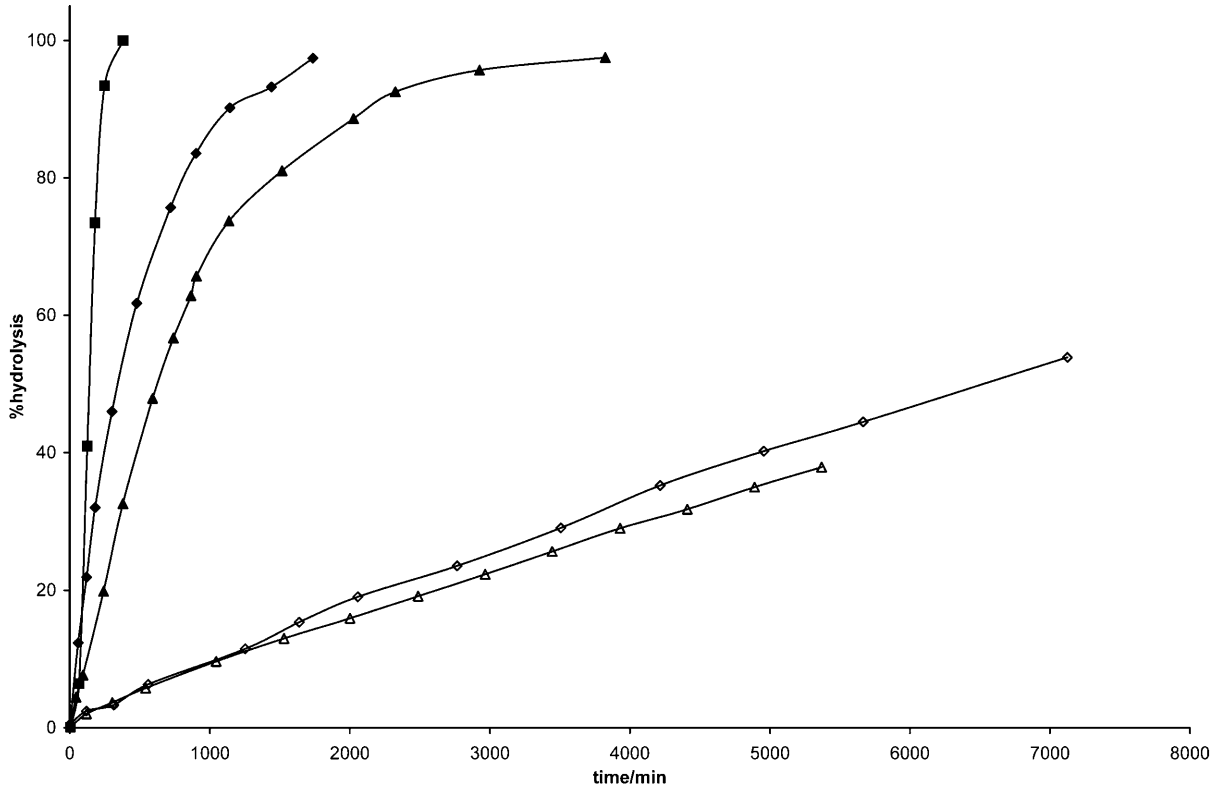

Figure 8. Plots of hydrolysis vs. reaction time for $[Ti(Ph^{tBu}N^{Me})_2(O^{iPr})_2]$ (■), $[Ti(Ph^{F}N^{Me})_2(O^{iPr})_2]$ (◆), $[Ti(Ph^{Me}N^{Me})_2(O^{iPr})_2]$ (▲), $[Ti(Ph^{Cl}N^{Me})_2(O^{iPr})_2]$ (◇), $[Ti(Ph^{Br}N^{Me})_2(O^{iPr})_2]$ (△). Data acquired by time-resolved ^{1}H NMR spectroscopy at 37 °C. Data gathered by monitoring the decrease in isolated signals of the titanium-bound salan backbone and the increase in the signals from the liberated alkoxy ligands. Integrals are normalized against the internal standard.

It is worth noting that X-ray structure determination revealed remarkably little difference between the chloro and the fluoro complexes ($[Ti(Ph^{F,Cl}N^{Me})_2(O^{iPr})_2]$). These complexes have comparable angles and distances around the titanium center (Table 7, Figure 9) and differ by only a $\delta =$ 0.3 ppm shift of the aromatic protons in the ^{1}H NMR spectra, so the reason for the enormous difference in hydrolytic stability remains unclear.

In a second set of experiments, we investigated the influence of different alkoxy ligands on the rate of hydrolysis. We supposed the alkoxides to have a rather big effect on the hydrolysis behavior compared with the substituents at the aromatic rings because they are in the vicinity of the metal center. Therefore, complexes $[Ti(Ph^{Me}N^{Me})_2(O^{a-d})_2]$ were exposed to the same hydrolysis conditions described above.

Keeping the different cytotoxicities of these complexes in mind, we were surprised to find that all four complexes resulted in the formation of the same degradation products upon hydrolysis (Figure 10). Interestingly, virtually no free ligand was observed (Figure 11).

Time-resolved ^{1}H NMR spectroscopy revealed that in the process of hydrolysis the distribution of the evolving products does not change over time. Figure 11 shows NMR spectra of the aromatic region of $[Ti(Ph^{Me}N^{Me})_2(O^{Et})_2]$ recorded at different times.

Table 7. Selected bond lengths [Å] and angles [°] for $[Ti(Ph^{F}N^{Me})_2(O^{iPr})_2]$ and $[Ti(Ph^{Cl}N^{Me})_2(O^{iPr})_2]$.

	$[Ti(Ph^{F}N^{Me})_2(O^{iPr})_2]$	$[Ti(Ph^{Cl}N^{Me})_2(O^{iPr})_2]$
Ti1−O1	1.9081(13)	1.904(2)
Ti1−O2	1.9315(13)	1.930(2)
Ti1−O3	1.8204(12)	1.8031(19)
Ti1−O4	1.7989(12)	1.7945(18)
Ti1−N1	2.3336(14)	2.339(2)
Ti1−N2	2.3425(14)	2.336(2)
O4-Ti1-O3	106.04(6)	106.76(9)
O4-Ti1-O1	97.17(5)	97.49(9)
O3-Ti1-O1	92.82(5)	93.19(9)
O4-Ti1-O2	92.45(5)	91.80(9)
O3-Ti1-O2	95.72(5)	96.36(9)
O1-Ti1-O2	164.87(5)	164.19(8)
O4-Ti1-N1	163.06(5)	162.89(8)
O3-Ti1-N1	90.36(5)	89.58(8)
O1-Ti1-N1	86.01(5)	86.40(8)
O2-Ti1-N1	81.47(5)	81.11(8)
O4-Ti1-N2	87.87(5)	88.15(8)
O3-Ti1-N2	165.49(5)	164.46(8)
O1-Ti1-N2	81.13(5)	80.23(8)
O2-Ti1-N2	87.61(5)	87.34(8)
N1-Ti1-N2	76.14(5)	76.04(8)

To estimate the influence of the different labile ligands on the half-life of the complexes, the change in intensity of distinct signals was monitored. Signals were chosen so that

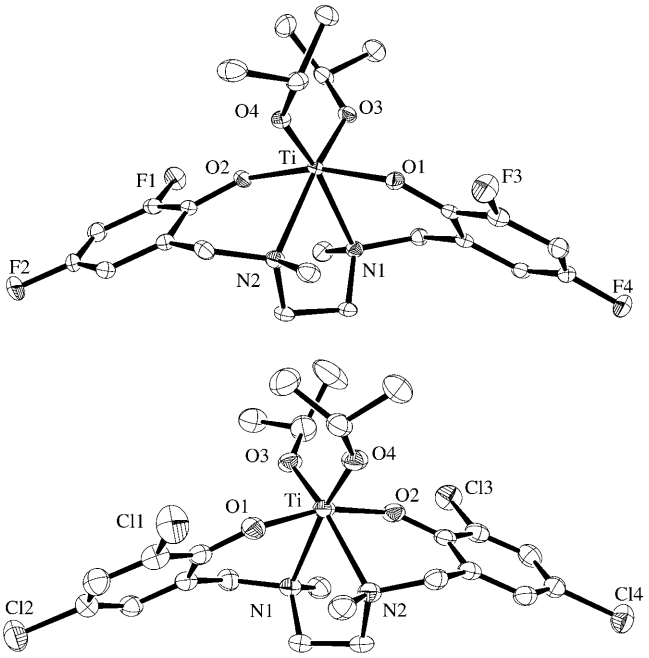

Figure 9. ORTEP diagrams of the molecular structures of $[Ti(Ph^{F}N^{Me})_2(O^{iPr})_2]$ (top) and $[Ti(Ph^{Cl}N^{Me})_2(O^{iPr})_2]$ (bottom). Displacement ellipsoids are drawn at the 50% probability level. Hydrogen atoms are omitted for clarity.

their integral ratios stayed constant relative to each other during the process of hydrolysis. This measure effectively excluded a possible overlay with signals of newly formed species.

The decreasing integrals of both the titanium-bound alkoxides and salan backbone and the increase in the evolving signals of the free alkoxy ligands were then normalized by using the DMSO signal as the internal standard and plotted against the hydrolysis time. Results for complexes $[Ti(Ph^{Me}N^{Me})_2(O^{a-d})_2]$ are given in Figure 12.

On comparing the hydrolysis rate of different alkoxides, a dependence on the steric demand of the labile ligand was observed (Table 8). In particular, complexes with alkoxides branched at C1, such as isopropanolate and *tert*-butanolate, displayed significantly faster hydrolysis than complexes with linear alkoxides, such as ethanolate or *n*-butanolate. When the cytotoxicity of the two complexes with branched alkoxides was compared, a decrease of one order of magnitude was observed despite very similar rates of hydrolysis. For complexes with similar IC_{50} values, the difference in rate of hydrolysis is, in the case of $[Ti(Ph^{Me}N^{Me})_2(O^{Et})_2]$ and $[Ti(Ph^{Me}N^{Me})_2(O^{iPr})_2]$, quite pronounced.

However, the difference in the rate of hydrolysis between $[Ti(Ph^{Me}N^{Me})_2(O^{iPr})_2]$ and its *tert*-butoxy counterpart is

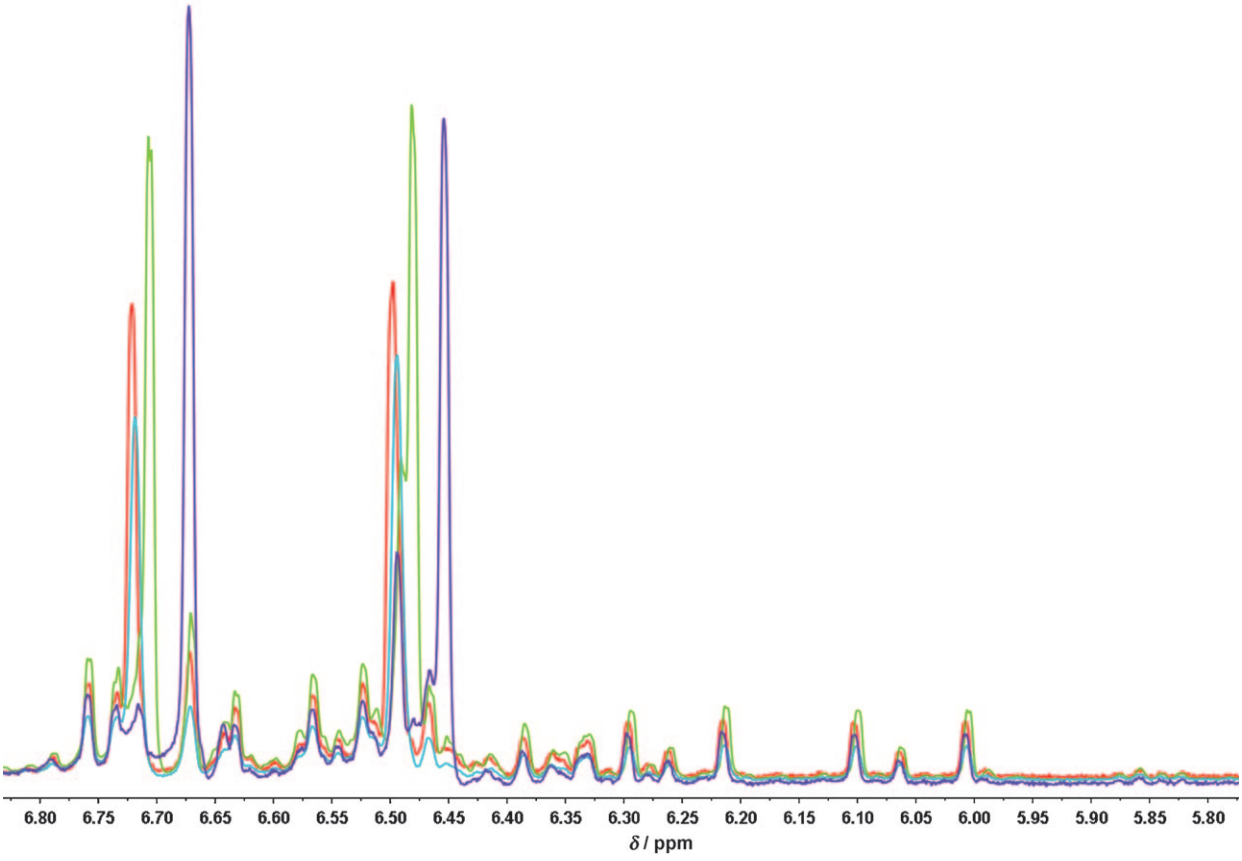

Figure 10. Superimposed ^1H NMR spectra of the aromatic region of $[Ti(Ph^{Me}N^{Me})_2(O^{Et})_2]$ (——), $[Ti(Ph^{Me}N^{Me})_2(O^{iPr})_2]$ (——), $[Ti(Ph^{Me}N^{Me})_2(O^{nBu})_2]$ (——), and $[Ti(Ph^{Me}N^{Me})_2(O^{tBu})_2]$ (——) at their respective $t_{1/2}$ values in the hydrolysis studies. Large signals arise from unhydrolysed complexes, small signals arise from hydrolysis products. No difference in the obtained products was observed.

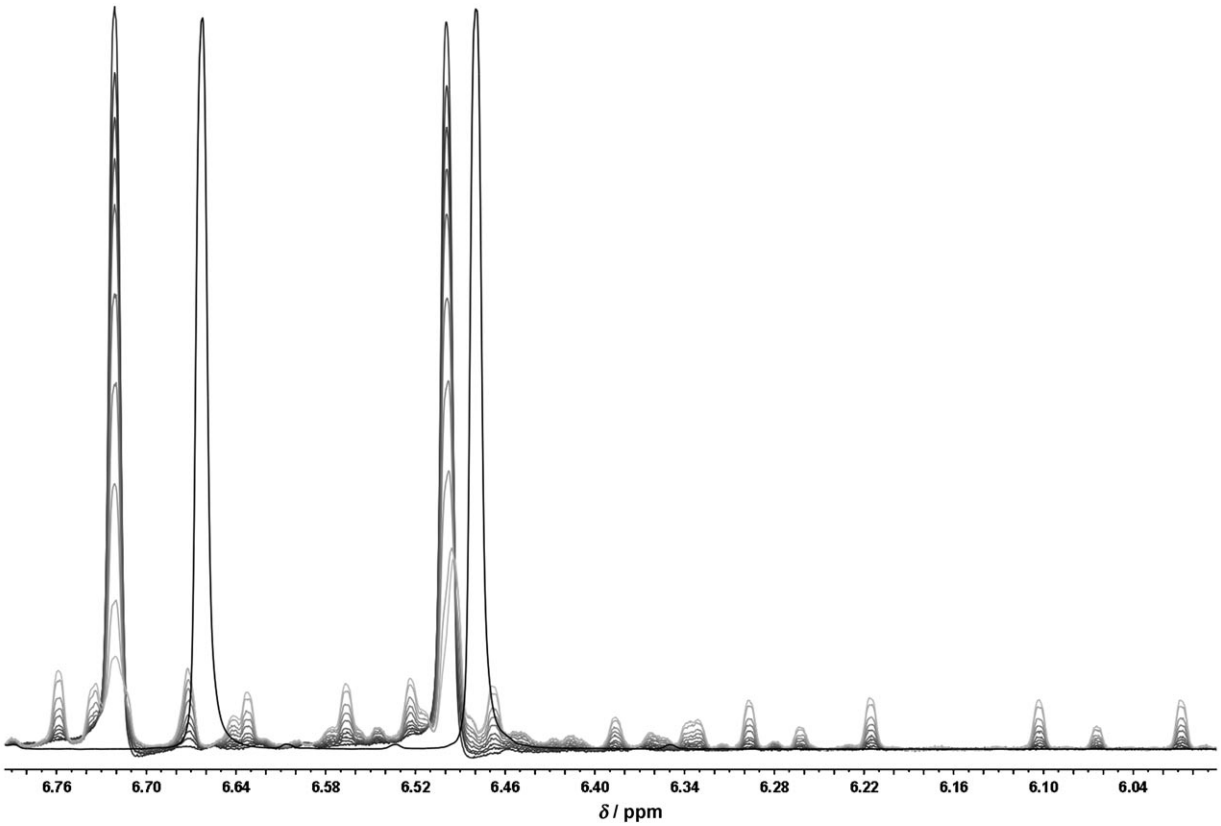

Figure 11. Multiple ^{1}H NMR spectra of the aromatic region of $[Ti(Ph^{Me}N^{Me})_2(O^{Et})_2]$ after 0, 3, 5, 7.5, 10, 15, 20, 30, 45, and 60 h (black→grey). Superimposition shows the unchanged distribution of hydrolysis products over time. The spectrum of the $(Ph^{Me}N^{Me})_2$ ligand (bold) is also shown for comparison.

rather small at 3 h. This does not reflect the rather drastic change in biological activity. Interestingly, the X-ray structure of $[Ti(Ph^{Me}N^{Me})_2(O^{tBu})_2]$ showed a alkoxy–titanium bond of 1.78 Å, which is shorter than complexes with unbranched alkoxides ($[Ti(Ph^{Me}N^{Me})_2(O^{Et})_2]$ 1.83 Å, $[Ti(Ph^{Me}N^{Me})_2(O^{nBu})_2]$ 1.82 Å). Nevertheless, this stronger O–Ti bond does not result in enhanced hydrolytic stability. Furthermore, the formation of the same degradation products indicates a similar mechanism of hydrolysis. Taking into account the fact that there is a difference of one order of magnitude in the cytotoxicity of these complexes, it seems implausible that hydrolysis functions as an activation mechanism. Activation via hydrolysis would require extremely different hydrolysis rates, which were not observed.

It seems that complexes with low IC_{50} values do not share a common hydrolytic profile and neither do nontoxic complexes. A certain rate of hydrolysis neither grants nor circumvents cytotoxicity in our experiments. Taken together with the earlier observed cross-relevance of the steric demand of salan and alkoxy ligand on cytotoxicity, our hydrolysis studies therefore strongly indicate that the unhydrolysed complex is important for the first interaction with a biomolecule. This does not rule out the possibility of hydrolytic deactivation of very unstable complexes.

Table 8. Comparison of half-life and IC_{50} values for complexes $[Ti(Ph^{Me}N^{Me})_2(O^{a-d})_2]$.[a]

	$[Ti(Ph^{Me}N^{Me})(O^{Et})_2]$	$[Ti(Ph^{Me}N^{Me})(O^{iPr})_2]$	$[Ti(Ph^{Me}N^{Me})(O^{nBu})_2]$	$[Ti(Ph^{Me}N^{Me})(O^{tBu})_2]$
$t_{1/2}$ [h]	18	10	16	7
Hela S3 IC_{50} [μM]	2.0±0.3	2.3±0.1	5.6±0.5	19.8±2.4
Hep G2 IC_{50} [μM]	1.6±0.3	2.1±0.1	5.2±0.5	26.9±8.6

[a] Hydrolysis was followed by time-resolved ^{1}H NMR spectroscopy at 37 °C, and cytotoxicities in Hela S3 and Hep G2 cells were determined by using an AlamarBlue assay after incubation for 48 h.

Seemingly, the determination of cytotoxicity by the steric demand of whole complexes and by inactivation via hydrolysis interferes with each other, but hydrolysis only plays a minor part within our complexes. This might be due to a slow hydrolysis compared with a much faster cellular uptake.

Conclusion

Herein, we present a library of more than 40 titanium salan complexes in which the steric demand of both the salan and the labile alkoxy ligands has been systematically altered. To enlighten the interconnection between steric demand, cytotoxicity, and hydrolytic behavior, all complexes were tested

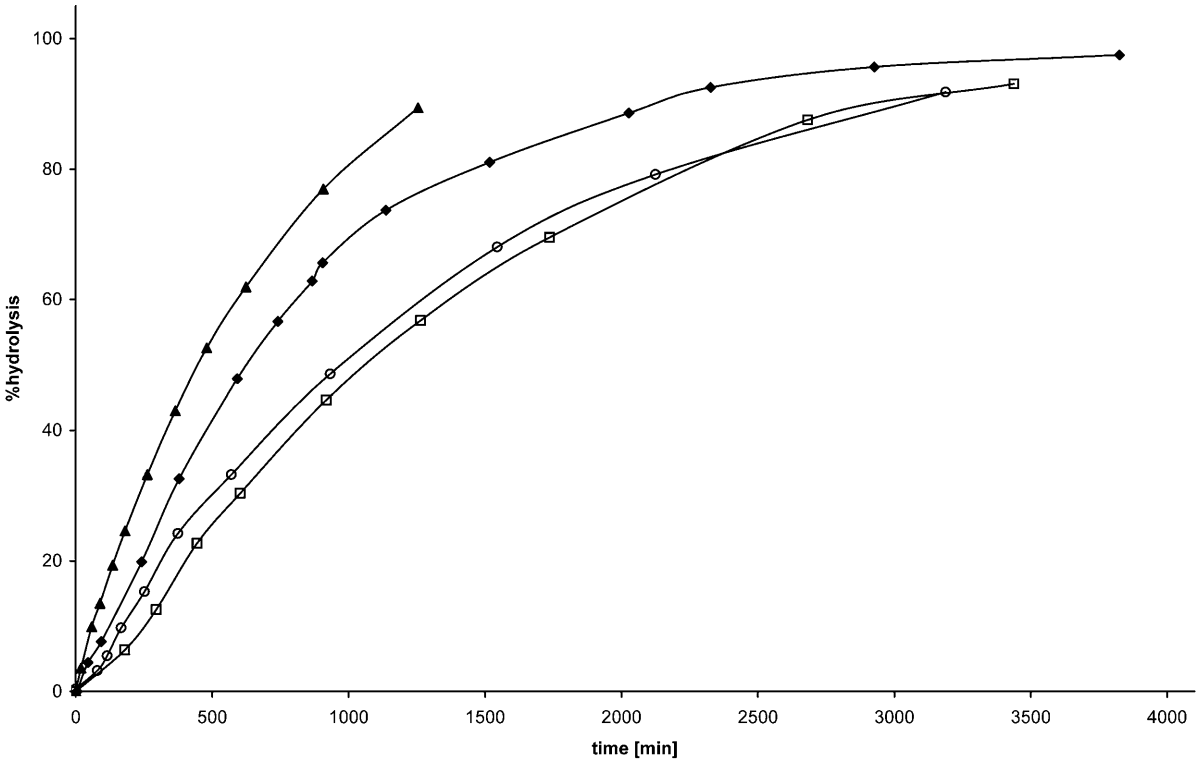

Figure 12. Plots of hydrolysis vs. reaction time for $[Ti(Ph^{Me}N^{Me})_2(O^{iBu})_2]$ (▲), $[Ti(Ph^{Me}N^{Me})_2(O^{iPr})_2]$ (◆), $[Ti(Ph^{Me}N^{Me})_2(O^{nBu})_2]$ (○), $[Ti(Ph^{Me}N^{Me})_2(O^{Et})_2]$ (□). Data acquired by time-resolved NMR spectroscopy at 37 °C.

on their biological activity and the hydrolysis of a selected set was followed by time-resolved ^{1}H NMR spectroscopy. It was already known that bulkier salan ligands result in less toxic complexes. Interestingly, we found that, in contrast to studies on titanocene derivatives, the exchange of the labile monodentate ligands can also have an enormous effect on cytotoxicity. However, not only did we find that the size of the alkoxy ligands is crucial for the cytotoxicity, but we also showed an interdependence of the steric demand of salan and alkoxy ligands. Very small salan ligands tolerated even the bulkiest of the alkoxides, *tert*-butoxide, without any loss of cytotoxicity. Complexes of medium-sized salans were extremely sensitive to even minor changes in the steric demand of the alkoxides. In this case, the respective complexes showed a stepwise decrease in cytotoxicity as the size of the alkoxide was increased. Finally, complexes of very bulky salans were nontoxic, even with the smallest labile ligand. We concluded that the overall size of the complexes determines their biological activity. This ligand–ligand interdependence also implies that the complex should be intact at the particular moment when the steric bulk determines the cytotoxicity of the complex. This result is especially unexpected because partial hydrolysis is believed to be an activation mechanism for many metal complexes. To investigate whether the overall steric demand itself alters the hydrolytic behavior of our complexes and, therefore, the cytotoxicity, hydrolysis experiments were conducted. We showed that complexes that only differed in their labile alkoxy ligands despite having very different cytotoxicities resulted in the same hydrolysis products and displayed only slightly varying $t_{1/2}$ values. Moreover, the distribution of the evolving products does not change over time. Therefore, we concluded that the active species is not a hydrolysis product. This supports our hypothesis of an important role for the intact complex and leads to the conclusion that hydrolysis is not an activation but a deactivation mechanism. The unhydrolyzed complex seems to be important for the first interaction with a biomolecule. Whether this is essential to transport the complex into the cell, for the portage to the as-yet unknown cellular target inside the cell, or the interaction at the site of action remains an open question for further studies.

Because our results promote the idea of hydrolysis being a detoxification pathway, we also screened our library for bioactive and highly stable complexes. Hydrolysis and the fast formation of unidentifiable byproducts have hampered the investigation of the mechanism of action of all titanium complexes found so far. Thus, such complexes might not only have an improved pharmacological profile, but also would be valuable tools for biochemical research. Therefore, we were happy to find a chloro-substituted complex that displayed rather high toxicity ($IC_{50} \approx 5\,\mu M$) and surprisingly high hydrolytic stability. With a hydrolytic half-life of 108 h, this complex showed a stability over 10 times higher than the most stable cytotoxic complex of this class known so far. When combined with its enhanced selectivity in inducing apoptosis,[43] the stability of this complex in aqueous media makes it one of the most promising substances in the field of anticancer titanium complexes.

Experimental Section

Materials and Methods: Syntheses of ligands $(Ph^{a-f}N^{Me})_2$[43,44] and $(Ph^{b,e}N^{Bn})_2$[45] were performed as described previously. Complexes $[Ti(Ph^{a-f}N^{Me})_2(O^{iPr})_2]$ were synthesized according to literature procedures.[43,46,47]

Titanium tetra(isopropoxide) (97%) and *N,N′*-dibenzylethylenediamine (97%) were purchased from Aldrich. Titanium tetra(ethoxide) (99%), titanium tetra(*n*-butoxide) (98%) and *N,N′*-diethylethylenediamine (96%) were purchased from ABCR (Karlsruhe, Germany); titanium tetra(*tert*-butoxide) (99%) and *N,N′*-dimethylethylenediamine (85%) were purchased from Acros Organics (Geel, Belgium). Deuterated solvents where purchased from Euriso-Top (Saarbrücken, Germany) in sealed ampoules and dried if necessary; other solvents were purified according to standard procedures.[53] All experiments requiring a dry atmosphere were carried out under nitrogen by using Schlenk techniques. NMR spectra were measured by using JEOL Eclipse 400 and Bruker Avance DRX 600 spectrometers. Structure assignments were done based on 2D NMR experiments (COSY, HMBC, HSQC).

The data collection for the X-ray structures was performed by using a STOE IPDS-II diffractometer equipped with a graphite monochromated radiation source ($\lambda = 0.71073$ Å), an image plate detection system, and an Oxford Cryostream 700 with nitrogen as the coolant gas. The selection, integration, and averaging procedure of the measured reflection intensities, the determination of the unit cell by a least-squares fit of the 2θ values, data reduction, LP correction, and the space group determination were performed by using the X-Area software package delivered with the diffractometer. A semiempirical absorption correction method was performed after indexing of the crystal faces. The structures were solved by direct methods (SHELXS-97)[54] and refined by standard Fourier techniques against F^2 with a full-matrix least squares algorithm by using SHELXL-97[54] and the WinGX (1.80.05)[55] software package. All nonhydrogen atoms were refined anisotropically. Hydrogen atoms were placed in calculated positions and refined with a riding model. Graphical representations were prepared with ORTEP-III.[56] CCDC-739047 ($[Ti(Ph^{Me}N^{Me})_2(O^{Et})_2]$), -739048 ($[Ti(Ph^{Me}N^{Me})_2(O^{tBu})_2]$), -739049 ($[Ti(Ph^{Me}N^{Me})_2(O^{nBu})_2]$),-739050 ($[Ti(Ph^{Cl}N^{Me})_2(O^{iPr})_2]$) and -719706 ($[Ti(Ph^{F}N^{Me})_2(O^{iPr})_2]$) contain the supplementary crystallographic data for this paper. These data can be obtained free of charge from The Cambridge Crystallographic Data Centre via www.ccdc.cam.ac.uk/data_request/cif. A summary of the relevant crystallographic data for this paper is shown in Table 9.

Hydrolysis experiments followed by NMR spectroscopy were conducted in a $[D_8]$THF (95%)/D_2O (4.8%)/DMSO (0.2%) mixture. The DMSO signal was used as the internal standard for calibrating the integrals. Spectra were recorded in 4 min intervals. Elemental analyses were performed at the microanalytical laboratory of the University of Konstanz. Cytotoxicity was measured on HeLa S3 and Hep G2 cells by using the AlamarBlue assay. The cells were cultivated at 37°C under humidified 5% CO_2 in Dulbecco's modified Eagle medium (Invitrogen) that contained 10% foetal calf serum, 1% penicillin, and 1% streptomycin, and were tested for mycoplasma infections by using a mycoplasma detection kit (Roche Applied Science, Mannheim, Germany) prior to use.

Peri et al. showed recently that the toxicity of the uncomplexed alkyl-substituted salans plays only a minor role in estimating complex toxicity.[40] By using flow cytometry (PI/annexin-FITC staining), we demonstrated the negligible cytotoxicity of the halo-substituted salans case as well.[43]

General procedure for synthesis of the ligands: 2,4-disubstituted phenol (10 mmol) was suspended or dissolved in methanol (5 mL), then formaldehyde (7.5 mL, 36% in water) and *N,N′*-disubstituted ethylenediamine (5 mmol) were added immediately. The mixture was heated at reflux for 24 h. Upon cooling, the ligands crystallized as colorless solids (47–61% yield).

General procedure for synthesis of the complexes: The ligand (1.5 mmol) was dissolved in toluene (10 mL), then titanium alkoxide (1.5 mmol) was added over a 10 min period under a nitrogen atmosphere. The resultant yellow reaction mixture was stirred overnight at RT. The solvent was removed under reduced pressure and the complex was obtained as a yellow solid (>90% yield). The crude product was recrystallized by using the procedure given in the Supporting Information.

Characterization data for new compounds and details of cell cultivation and cytotoxicity studies in HeLa S3 and Hep G2 cells are given in the Supporting Information.

Table 9. Crystallographic data for complexes $[Ti(Ph^{Me}N^{Me})_2(O^{a,c,d})_2]$, $[Ti(Ph^{F}N^{Me})_2(O^{iPr})_2]$, and $[Ti(Ph^{Cl}N^{Me})_2(O^{iPr})_2]$.

	$[Ti(Ph^{Me}N^{Me})_2(O^{Et})_2]$	$[Ti(Ph^{Me}N^{Me})_2(O^{nBu})_2]$	$[Ti(Ph^{Me}N^{Me})_2(O^{tBu})_2]$	$[Ti(Ph^{F}N^{Me})_2(O^{iPr})_2]$	$[Ti(Ph^{Cl}N^{Me})_2(O^{iPr})_2]$
formula	$C_{26}H_{40}N_2O_4Ti$	$C_{30}H_{48}N_2O_4Ti$	$C_{30}H_{48}N_2O_4Ti$	$C_{24}H_{32}F_4N_2O_4Ti$	$C_{24}H_{32}Cl_4N_2O_4Ti$
M_r	492.50	548.60	548.60	536.39	602.22
crystal size [mm³]	0.55×0.35×0.1	0.55×0.4×0.05	0.6×0.5×0.2	0.5×0.35×0.15	0.3×0.3×0.3
crystal system	monoclinic	monoclinic	monoclinic	monoclinic	monoclinic
space group	*P*21/*c*	*P*21/*c*	*P*21/*c*	*P*21/*c*	*P*21/*c*
a [Å]	11.7789(7)	11.4262(7)	17.5177(18)	8.2933(4)	9.270(4)
b [Å]	16.9074(10)	15.4592(6)	9.9728(6)	12.6602(7)	12.783(4)
c [Å]	13.1780(8)	17.2942(10)	18.3729(19)	23.7332(10)	23.673(6)
α [°]	90.00	90.00	90.00	90.00	90.00
β [°]	105.661(5)	107.064(5)	109.273(8)	95.308(3)	95.31(2)
γ [°]	90.00	90.00	90.00	90.00	90.00
V [Å³]	2527.0(3)	2920.4(3)	3029.9(5)	2481.2(2)	2793.3(16)
Z	4	4	4	4	4
ρ_{calc} [g cm⁻³]	1.295	1.248	1.203	1.436	1.432
T [K]	100(2)	100(2)	100(2)	100(2)	373(2)
$\mu(Mo_{K\alpha})$ [mm⁻¹]	0.372	0.329	0.317	0.408	0.721
F(000)	1056	1184	1184	1120	1248
θ range [°]	1.80–25.81	1.3–28.4	2.26–26.21	1.72–26.88	1.2–15.13
reflns collected	32883	37408	26501	35513	6483
indep. reflns (R_{int})	4870 (0.0986)	8771 (0.0719)	6080 (0.1301)	5363 (0.0661)	6103 (0.0322)
data/restraints/param	4784/0/298	8688/0/342	6077/54/368	5273/0/316	6103/0/322
GOF on F^2	1.023	0.975	0.988	1.063	1.085
R_1, wR_2 [$I>2\sigma(I)$]	4.86, 10.88	5.25, 10.24	6.97, 13.42	3.46, 8.74	4.00, 9.05
R_1, wR_2 (all data)	7.63, 11.74	9.75, 11.45	14.17, 15.92	4.69, 9.61	6.34, 11.29
largest diff. peak/hole [e Å⁻³]	0.412/−0.365	0.444/−0.289	0.339/−0.388	0.274/−0.525	0.694/−0.332

Acknowledgements

The authors would like to thank the Konstanz Research School Chemical Biology (KoRS-CB) for financial and scientific support. T.A.I. thanks the KoRS-CB for a personal scholarship. The authors would also like to thank Dr. Malgorzata Debiak for providing the cisplatin-resistant and -hypersensitive cell lines, Dipl.-chem. Malin Bein for help with the biological assays, Anke Friemel for recording the time-resolved and 2D NMR spectroscopy data, Martin Luka and Dominik Fröhlich for the synthesis of several precursors, and Dr. Michael Burgert for solving the X-ray structures.

[1] E. Wong, C. M. Giandomenico, *Chem. Rev.* **1999**, *99*, 2451–2466.
[2] M. A. Jakupec, M. Galanski, B. K. Keppler, *Rev. Physiol. Biochem. Pharmacol.* **2003**, *146*, 1–54.
[3] M. Galanski, M. A. Jakupec, B. K. Keppler, *Curr. Med. Chem.* **2005**, *12*, 2075–2094.
[4] M. Coluccia, G. Natile, *Anti-Cancer Agents Med. Chem.* **2007**, *7*, 111–123.
[5] P. C. A. Bruijnincx, P. J. Sadler, *Curr. Opin. Chem. Biol.* **2008**, *12*, 197–206.
[6] M. A. Jakupec, M. Galanski, V. B. Arion, C. G. Hartinger, B. K. Keppler, *Dalton Trans.* **2008**, 183–194.
[7] M. J. Clarke, F. Zhu, D. R. Frasca, *Chem. Rev.* **1999**, *99*, 2511–2534.
[8] M. Galanski, V. B. Arion, M. A. Jakupec, B. K. Keppler, *Curr. Pharm. Des.* **2003**, *9*, 2078–2089.
[9] B. Desoize, *Anticancer Res.* **2004**, *24*, 1529–1544.
[10] I. Ott, R. Gust, *Arch. Pharm. Chem. Life Sci.* **2007**, *340*, 117–126.
[11] N. Katsaros, A. Anagnostopoulou, *Crit. Rev. Oncol. Hematol.* **2002**, *42*, 297–308.
[12] A. M. Evangelou, *Crit. Rev. Oncol. Hematol.* **2002**, *42*, 249–265.
[13] I. Kostova, *Curr. Med. Chem.* **2006**, *13*, 1085–1107.
[14] I. Kostova, *Anticancer Agents Med. Chem.* **2006**, *6*, 19–32.
[15] F. Caruso, M. Rossi, *Mini-Rev. Med. Chem.* **2004**, *4*, 49–60.
[16] E. Melendez, *Crit. Rev. Oncol. Hematol.* **2002**, *42*, 309–315.
[17] E. Y. Tshuva, D. Peri, *Coord. Chem. Rev.* **2009**, *253*, 2098–2115.
[18] H. Köpf, P. Köpf-Maier, *Angew. Chem.* **1979**, *91*, 509; *Angew. Chem. Int. Ed. Engl.* **1979**, *18*, 477–478.
[19] P. Köpf-Maier, F. Preiss, T. Marx, T. Klapötke, H. Köpf, *Anticancer Res.* **1986**, *6*, 33–37.
[20] N. J. Sweeney, O. Mendoza, H. Müller-Bunz, C. Pampillón, F.-J. K. Rehmann, K. Strohfeldt, M. Tacke, *J. Organomet. Chem.* **2005**, *690*, 4537–4544.
[21] P. M. Abeysinghe, M. M. Harding, *Dalton Trans.* **2007**, 3474–3482.
[22] K. Strohfeldt, M. Tacke, *Chem. Soc. Rev.* **2008**, *37*, 1174–1187.
[23] F. Caruso, M. Rossi, J. Tanski, R. Sartori, R. Sariego, S. Moya, S. Diez, E. Navarrete, A. Cingolani, F. Marchetti, C. Pettinari, *J. Med. Chem.* **2000**, *43*, 3665–3670.
[24] T. Schilling, K. B. Keppler, M. E. Heim, G. Niebch, H. Dietzfelbinger, J. Rastetter, A. R. Hanauske, *Invest. New Drugs* **1996**, *14*, 327–332.
[25] H. Bischoff, M. R. Berger, B. K. Keppler, D. Schmähl, *J. Cancer Res. Clin. Oncol.* **1987**, *113*, 446–450.
[26] J. H. Toney, T. J. Marks, *J. Am. Chem. Soc.* **1985**, *107*, 947–953.
[27] H. Köpf, S. Grabowski, R. Voigtländer, *J. Organomet. Chem.* **1981**, *216*, 185–190.
[28] P. Köpf-Maier, *Eur. J. Clin. Pharmacol.* **1994**, *47*, 1–16.
[29] C. V. Christodoulou, A. G. Eliopoulos, L. S. Young, L. Hodgkins, D. R. Ferry, D. J. Kerr, *Br. J. Cancer* **1998**, *77*, 2088–2097.
[30] M. Guo, Z. Guo, P. J. Sadler, *J. Biol. Inorg. Chem.* **2001**, *6*, 698–707.
[31] G. Mokdsi, M. M. Harding, *J. Organomet. Chem.* **1998**, *565*, 29–35.
[32] G. Mokdsi, M. M. Harding, *J. Inorg. Biochem.* **2001**, *83*, 205–209.
[33] H. Sun, H. Li, R. A. Weir, P. J. Sadler, *Angew. Chem.* **1998**, *110*, 1622–1625; *Angew. Chem. Int. Ed.* **1998**, *37*, 1577–1579.
[34] M. Guo, H. Sun, H. J. McArdle, L. Gambling, P. J. Sadler, *Biochemistry* **2000**, *39*, 10023–10033.
[35] L. M. Gao, R. Hernandez, J. Matta, E. Melendez, *J. Biol. Inorg. Chem.* **2007**, *12*, 959–967.
[36] A. D. Tinoco, A. M. Valentine, *J. Am. Chem. Soc.* **2005**, *127*, 11218–11219.
[37] A. D. Tinoco, C. D. Incarvito, A. M. Valentine, *J. Am. Chem. Soc.* **2007**, *129*, 3444–3454.
[38] A. D. Tinoco, E. V. Eames, A. M. Valentine, *J. Am. Chem. Soc.* **2008**, *130*, 2262–2270.
[39] M. Shavit, D. Peri, C. M. Manna, J. S. Alexander, E. Y. Tshuva, *J. Am. Chem. Soc.* **2007**, *129*, 12098–12099.
[40] D. Peri, S. Meker, M. Shavit, E. Y. Tshuva, *Chem. Eur. J.* **2009**, *15*, 2403–2415.
[41] E. Y. Tshuva, D. Peri, *Coord. Chem. Rev.* **2009**, *253*, 2098–2115.
[42] E. Y. Tshuva, J. A. Ashenhurst, *Eur. J. Inorg. Chem.* **2009**, 2203–2218.
[43] T. A. Immel, M. Debiak, U. Groth, A. Bürkle, T. Huhn, *ChemMedChem.* **2009**, *4*, 738–741.
[44] E. Y. Tshuva, N. Gendeziuk, M. Kol, *Tetrahedron Lett.* **2001**, *42*, 6405–6407.
[45] P. Hormnirun, E. L. Marshall, V. C. Gibson, A. J. P. White, D. J. Williams, *J. Am. Chem. Soc.* **2004**, *126*, 2688–2689.
[46] J. Balsells, P. J. Carroll, P. Walsh, *Eur. J. Inorg. Chem.* **2001**, 5568–5574.
[47] S. Gendler, S. Segal, I. Goldberg, Z. Goldschmidt, M. Kol, *Inorg. Chem.* **2006**, *45*, 4783–4790.
[48] R. Hamid, Y. Rotshteyn, L. Rabadi, R. Parikh, P. Bullock, *In Vitro Toxicol.* **2004**, *18*, 703–710.
[49] S. N. MacMillan, C. F. Jung, T. Shalumova, J. M. Tanski, *Inorg. Chim. Acta* **2009**, *362*, 3134–3146.
[50] P. Köpf-Maier, B. Hesse, R. Voigtländer, H. Köpf, *J. Cancer Res. Clin. Oncol.* **1980**, *97*, 31–39.
[51] J. R. Boyles, M. C. Baird, B. G. Campling, N. Jain, *J. Inorg. Biochem.* **2001**, *84*, 159–162.
[52] NMR spectra are depicted in the Supporting Information.
[53] W. L. F. Armarego, C. L. L. Chai, *Purification of Laboratory Chemicals*, 5th ed., Elsevier, Amsterdam, **2003**.
[54] G. M. Sheldrick, SHELX-97, University of Göttingen, Göttingen, **1997**.
[55] L. J. Farrugia, *J. Appl. Crystallogr.* **1999**, *32*, 837–838.
[56] ORTEP-III for Windows, L. J. Farrugia, *J. Appl. Crystallogr.* **1997**, *30*, 565.

Received: August 20, 2009
Published online: January 26, 2010

